energies

MDPI

Article

A Diagnosis Method of Power Flow Convergence Failure for Bulk Power Systems Based on Intermediate Iteration Data

Gang Mu, Yibo Zhou *, Mao Yang and Jiahao Chen

Key Laboratory of Modern Power System Simulation and Control & Renewable Energy Technology, Ministry of Education, Northeast Electric Power University, Jilin City 132012, China; 18844216892@163.com (J.C.)
* Correspondence: zhouyiboaa@126.com

Abstract: Power flow calculation is the foundation of security analyses in a power system, and the phenomenon of convergence failure is becoming more prominent with the expansion of the power grid. The existing convergence failure diagnosis methods based on optimization modeling and local feature recognition are no longer viable for bulk power systems. This paper proposes a diagnosis method based on intermediate iteration data and the identification of the transmission power congested channel. Firstly, the transmission power congestion index is constructed, and then a method for identifying transmission congestion channels is proposed. The reasons for convergence failure of the power flow are diagnosed from two aspects: excessive power to be transmitted and insufficient transmission capacity. Finally, with the aim of alleviating transmission channel congestion, a correction strategy for power flow injection space data was constructed, which generates relaxation schemes for operational variables. The effectiveness of the proposed strategy was verified using the simulation results of an actual provincial power grid and a standard example power system with 13,659 buses. The method proposed in this paper is entirely based on intermediate power flow iteration data, which avoids the complex modeling of the power flow adjustment and provides methodological support for power flow diagnosis in bulk power systems.

Keywords: power flow convergence failure; intermediate iteration data; diagnosis; power flow adjustment; transmission power congestion

Citation: Mu, G.; Zhou, Y.; Yang, M.; Chen, J. A Diagnosis Method of Power Flow Convergence Failure for Bulk Power Systems Based on Intermediate Iteration Data. *Energies* **2023**, *16*, 3540. https://doi.org/10.3390/en16083540

Academic Editors: Jing Zhang, Bi Liu, Rujing Yan and Xiao Xu

Received: 24 March 2023
Revised: 8 April 2023
Accepted: 18 April 2023
Published: 19 April 2023

1. Introduction

As the penetration of renewable energy sources continues to increase in bulk power systems, the operation modes of power systems are becoming more diverse. To ensure the safety of power grid operation, it is necessary to arrange and verify the operation modes of the power grid while considering the simultaneity of renewable energy generation output in various scenarios. In this process, the power flow calculation often fails to converge.

Due to the complex factors leading to power flow convergence failure, the diagnostic information provided by non-convergent power flows is limited. Faced with non-convergent power flow calculation results, power grid operators lack systematic and targeted solutions and can only try to adjust the given control variables or grid structure parameters based on experience. This manual diagnostic method is time-consuming, labor-intensive, and usually requires adjustments to a large number of variables [1–5]. Therefore, it is of great importance to carry out research on automatic diagnosis methods and the adjustment of power flow convergence failure.

If the convergence failure caused by an incomplete algorithm for solving power flow equations is not considered, relaxing the specified injection conditions appropriately becomes an effective means to solve the problem of power flow convergence failure [6–10]. Some experts and scholars have proposed to establish an optimization model for control variables and use optimization theory to calculate the power flow results under appropriate relaxation conditions [11,12]. Based on this idea, optimization algorithms represented

by the interior point method are widely used in power flow convergence adjustment due to their high computational efficiency and fast solving speed [13,14]. However, the optimization model also has convergence difficulties when the system scale increases. Moreover, which control variables are relaxed and to what extent is entirely mathematical and is not based on the analysis of physical problems.

To achieve targeted power flow diagnosis and adjustment, [15,16] computed the normal direction of the convergence boundary of the power flow passing through the initial operating point and adjusted the infeasible control variables along the normal direction to make the power flow calculation converge. Reference [17] used the output reduction method to find the weak voltage channels in the system and propose a practical power flow adjustment method. Reference [18] pre-allocated the larger regional unbalanced active power in the given conditions of the power flow calculation, avoiding the non-convergence problem caused by excessive output of balancing machines from the perspective of power balance.

In recent years, some researchers have started to pay attention to diagnosing the causes of non-convergence by utilizing intermediate iteration data in power flow calculations. Reference [19] located key buses and variables based on the changing characteristics of the voltage phase angle during the iteration process and proposed a method for adjusting the ill-conditioned power flow. Reference [20] characterized the boundary of the power flow convergence domain using bus-injected active/reactive power during the iteration process and provided adjustment schemes for a non-converging power flow, but the convergence boundary in high-dimensional space was difficult to depict.

In previous studies, the existing research mainly concerns improved power-flow-solving algorithms and slacking methods for individual control variables. However, the current research has the following limitations:

1. For the research idea of generating a power flow calculation control variable relaxation scheme based on optimization model construction and the mathematical solution method, the cause of power flow convergence failure is ignored, and the selection of adjustment variables lacks specificity. Moreover, the adjustment may also fail due to the difficulty of solving the complex optimization model in bulk power systems;
2. Current research is more concerned with local variables causing power flow convergence failure. The non-convergence of power flow is usually a global power balance problem, and strategies that only depend on local variable adjustment may fail.

The existing convergence failure diagnosis methods based on optimization modeling and local feature recognition are no longer viable in bulk power systems. However, the intermediate iteration data contain abundant diagnostic information about power flow convergence failure, and the intermediate data of power flow have not been fully utilized. The highlights and main contributions of this paper are as follows:

1. We proposed a diagnosis and adjustment method that is entirely based on intermediate iteration data, which avoids complex modeling and problem-solving processes;
2. The causes of power flow convergence failure are revealed from the perspective of power congestion. The reasons for convergence failure are diagnosed from the aspects of excessive power to be transmitted and insufficient transmission capacity;
3. Aiming to alleviate transmission channel congestion, a power flow injection space data correction strategy is proposed, which automatically generates operation variable relaxation schemes.

The remaining chapters of this paper are as follows: Section 2 introduces the extraction method for intermediate power flows. Section 3 introduces the diagnosis method for the cause of non-convergence based on congestion theory. In Section 4, a convergence adjustment method based on intermediate power flow is presented. Section 5 describes the case analysis in an actual grid and the European 13,659-bus system, and Section 6 presents the conclusions obtained in this paper. Finally, Section 7 outlines a reasonable prospect for the future based on this paper.

2. Convergence Feature Extraction Based on Intermediate Power Flows

2.1. Introduction to the Intermediate Power Flow of Newton Class Iterative Methods

The power system load flow equations are a set of non-linear algebraic equations. The Newton–Raphson method is a typical representative of Newton-type algorithms. The core is to linearize the non-linear algebraic equation set and establish the correction equations for state variables. Then, after giving initial values, the solution is obtained iteratively step by step. The iteration formula is as follows:

$$\Delta F^{(k)} = J(X^{(k)})\Delta X^{(k)} \tag{1}$$

where $J(X^{(k)})$ represents the Jacobian matrix at the kth iteration, $\Delta X^{(k)}$ denotes the update step length of the state variables to be determined, and $\Delta F^{(k)} = F^{sp} - F(X^{(k)})$ refers to the iterative error of the control variables.

Thus, the imbalance quantity of the bus-injected power during the iterative process represents the deviation between the bus injection power calculated based on the state variables and the specified value when the state variables are at a certain intermediate iteration value, as shown in Equation (2).

$$\begin{cases} \Delta P_i^{(k)} = P_i^{sp} - P_i^{(k)} = P_i^{sp} - U_i^{(k)} \sum\limits_{j=1}^{n} U_j^{(k)} \left(G_{ij} \cos \theta_{ij}^{(k)} + B_{ij} \sin \theta_{ij}^{(k)} \right) \\ \Delta Q_i^{(k)} = Q_i^{sp} - Q_i^{(k)} = Q_i^{sp} - U_i^{(k)} \sum\limits_{j=1}^{n} U_j^{(k)} \left(G_{ij} \sin \theta_{ij}^{(k)} - B_{ij} \cos \theta_{ij}^{(k)} \right) \end{cases} \tag{2}$$

where P_i^{sp} and Q_i^{sp} represent the given bus injection power, U_i represents the voltage amplitude of bus i, and $\theta_{ij} = \theta_i - \theta_j$ represents the angle difference of the bus voltage.

Generally, the convergence process of the power flow calculation can be mathematically viewed as the process of continuously updating the state variables U and θ. Physically, it can also be explained as the process of continuously adjusting the power flow distribution with respect to U and θ, so that the injected power $P_i^{(k)}$ and $Q_i^{(k)}$ of each bus gradually approach P_i^{sp} and Q_i^{sp}. In each iteration, as show in [21], the injected power of each bus can be calculated using Equation (3).

$$\begin{cases} P_i^{(k)} = U_i^{(k)} \sum\limits_{j=1}^{n} U_j^{(k)} \left(G_{ij} \cos \theta_{ij}^{(k)} + B_{ij} \sin \theta_{ij}^{(k)} \right) \\ Q_i^{(k)} = U_i^{(k)} \sum\limits_{j=1}^{n} U_j^{(k)} \left(G_{ij} \sin \theta_{ij}^{(k)} - B_{ij} \cos \theta_{ij}^{(k)} \right) \end{cases} \tag{3}$$

Equation (3) reveals that the intermediate iterations in the power flow calculation also satisfy the physical constraint. Moreover, the topological and parameter information is completely consistent with the given conditions. Therefore, the intermediate results of the power flow calculation can also be regarded as a complete power flow, which is known as the intermediate power flow.

By adopting the concept of intermediate power flow, in each iteration of the power flow calculation process, it can provide complete information similar to the conventional converged power flow. This not only includes the bus voltage magnitude, the bus voltage angle, and the injected active and reactive power information in Equation (3), but also allows for obtaining the power distribution characteristics on each branch through the intermediate power flow. The branch power calculation is shown in Equation (4).

$$\begin{cases} P_{ij}^{(k)} = U_i^{(k)} U_j^{(k)} \left(G_{ij} \cos \theta_{ij}^{(k)} + B_{ij} \sin \theta_{ij}^{(k)} \right) \\ Q_{ij}^{(k)} = U_i^{(k)} U_j^{(k)} \left(G_{ij} \sin \theta_{ij}^{(k)} - B_{ij} \cos \theta_{ij}^{(k)} \right) \end{cases} \tag{4}$$

The difference between the intermediate power flow and the original power flow lies in the fact that the bus-injected power changes from P_i^{sp} (Q_i^{sp}) to $P_i^{(k)}$ ($Q_i^{(k)}$). From a mathematical point of view, if the convergence accuracy threshold parameter is appropriately increased, and the error between the given P_i^{sp} (Q_i^{sp}) and the $P_i^{(k)}$ ($Q_i^{(k)}$) is within the allowable range, the power flow calculation can be considered to converge. However, from an engineering perspective, the contact buses of intermediate power flow may include no physically significant injected power, buses with excessively high or low voltage magnitude, large voltage angle differences, and generator buses with injected power exceeding the physical capacity. Therefore, the intermediate power flow cannot usually be directly used as the converged power flow in the original injection space.

In summary, for power flow calculations that do not converge in the original given space, the intermediate power flow maintains the characteristics of the original power system topology and parameters, and provides information such as the branch power flow, the bus voltage magnitude, and the bus voltage angle, which are difficult to obtain from the original non-convergent power flow, thus expanding the data sources for diagnosing the reasons for the non-convergence of power flow. In addition, the intermediate power flow is also affected by the values of the original control variables and reflects the characteristics of the original injection space. An in-depth exploration of the characteristics of the intermediate power flow can provide strong evidence for diagnosing the factors causing non-convergence of the original injection space.

2.2. Key Feature Extraction for Convergence Diagnosis Based on Intermediate Power Flow

For a power flow calculation with an initial injection space that does not converge, the evolution of the injection space of the intermediate power flow during the iteration process is shown in Figure 1. At the start of the power flow calculation, the state variables are given initial values, usually with an initial voltage magnitude $U^{(0)} = 1.0$ and an initial voltage angle $\theta^{(0)} = 0°$. Usually, the initial bus-injected power $(P^{(0)}, Q^{(0)})$ significantly differs from the given injection space (P^{sp}, Q^{sp}). As the iteration process proceeds, there must exist an m ($m \geq 1$) where the injection space $(P^{(m)}, Q^{(m)})$ of the intermediate power flow in the mth iteration is closest to the original given injection space (P^{sp}, Q^{sp}). This also means that the voltage magnitude and angle $(U^{(m)}, \theta^{(m)})$ of the intermediate power flow in the mth iteration are closest to the given injection space, which is a solvability condition for the power flow.

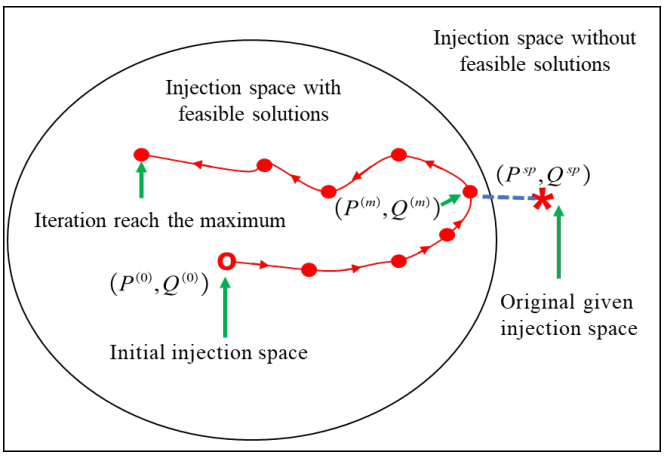

Figure 1. The evolution of the injection space of the intermediate power flow during the iteration process.

Based on the above analysis, it can be concluded that the intermediate power flow closest to the given injection space contains more diagnostic information about the convergence of the original injection space.

Since the control variable of the power flow calculation is the bus-injected power, which is a multi-dimensional vector, it is necessary to explore methods for quantitatively evaluating the distance between the intermediate power flow injection variables and the given original injection variables in high-dimensional space. Through extensive previous research, it was found that using the Euclidean geometric similarity evaluation metric can achieve good results, and the distance between different iterations can be expressed as follows:

$$L_k = \left\| \left\{ \Delta P_i^{(k)}, \Delta Q_i^{(k)} \right\}, i = 1, 2, \ldots, n \right\|_2 \tag{5}$$

Within the calculation results obtained from Equation (5), the intermediate power flow with the smallest distance can be selected. In the subsequent analysis, unless otherwise specified, the intermediate power flow refers to the power flow with the smallest distance.

Ignoring the unreasonable network structural parameters, the reason as to why the intermediate power flow cannot converge to the given bus injection conditions through continued iteration can be attributed to the fact that the initial injection space is unreasonable, which causes the power flow of the branch in the power grid to exceed the branch limit and, thus, be unable to deliver the specified amount of power.

The relationship between power transmission blockage and the convergence of intermediate power flow branches is illustrated using a single generator and single load system, as shown in Figure 2.

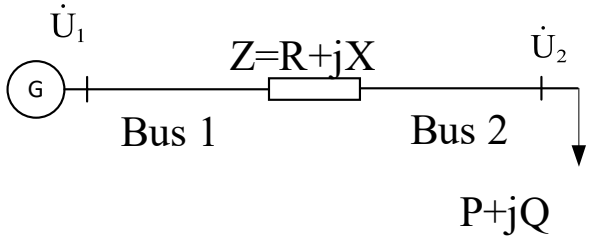

Figure 2. Single generator and single load system.

Assuming the voltage vectors of Bus 1 and 2 are $\dot{U}_1 = U_1 \angle 0^\circ$ and $\dot{U}_2 = U_2 \angle \theta$, respectively, and Bus 1 transfers power to Bus 2 through a transmission line with an impedance $Z = R + jX$, while Bus 2 has a load impedance that consumes power $\widetilde{S} = P + jQ$. Neglecting the admittance to ground, the power flow equation of the two-bus system can be expressed as follows:

$$\begin{cases} P = \frac{U_1 U_2}{Z} \cos(\theta + \delta) - \frac{U_2^2}{Z} \cos \delta \\ Q = \frac{U_1 U_2}{Z} \sin(\theta + \delta) - \frac{U_2^2}{Z} \sin \delta \end{cases} \tag{6}$$

where δ is the angle of the line impedance.

Assuming the power factor angle at the end of the line is φ, the active power P of the transmission line is formed as:

$$P = \frac{\cos \varphi}{Z} \left(-U_2^2 \cos(\delta - \varphi) + \sqrt{\left[U_2^2 \cos(\delta - \varphi) \right]^2 - U_2^4 + U_1^2 U_2^2} \right) \tag{7}$$

When the transferred active power reaches its limit, let $\frac{dP}{dU_2} = 0$, then Equation (8) is formed from Equation (7):

$$U_2 = \frac{U_1}{\sqrt{2[1 + \cos(\delta - \varphi)]}} \tag{8}$$

Substituting U_2 into Equation (7) yields the maximum transmission power of the branch:

$$P_{\max} = \frac{U_1^2 \cos\varphi}{2Z[1+\cos(\delta-\varphi)]} \tag{9}$$

From Equation (9), the following conclusions can be drawn:

(1) Assuming the branch impedance is constant, the maximum power transmitted through the branch is not fixed and can be increased by improving the power factor when the power factor angle is not taken as $-\delta$;
(2) The power transmission limit of the branch is proportional to the square of the voltage on the sending side. The power transmission capacity of the branch can be improved by increasing the voltage on the sending side while keeping the power factor constant;
(3) When the impedance and voltage of sending side are specified, $P_{\max}$ has a maximum value, and the actual value of the branch power must be less than this limit. The closer the transmitted power is to the limit, the more difficult it is for the power flow to converge.

Considering some extreme operating conditions, e.g., assuming that the voltage loss on the sending side of all branches does not exceed 20%, and the power factor of the receiving side is not less than 0.85, the relative transmission limit of the branch under this constraint can be approximately calculated by Equation (9), which is denoted as $\overline{P}_{\max}$. Compared to the mathematical maximum value $P_{\max}$, $\overline{P}_{\max}$ can provide a reference value for the branch transmission limit from the perspective of engineering, which is of great significance in distinguishing whether the convergence problem of power flow is caused by the unreasonable distribution of active power or reactive power.

3. A Diagnosis Method for the Cause of Non-Convergence Based on Congestion Theory

3.1. Diagnosis Indicators for Non-Convergence of Power Flow

As analyzed in Section 2.2, a branch power transmission metric based on intermediate power flow is proposed, and C_l is defined as follows:

$$C_l = 1 - \frac{|P_l|}{\overline{P}_{\max}} \tag{10}$$

where P_l represents the transmitted branch power through the intermediate power flow. In Equation (10), the smaller the value of, C_l the closer the transmitted power is to the power transmission limit of the branch. If the given variables in the power flow calculation are not relaxed at this point, the power flow calculation of the bulk power system will fail to converge due to partial power congestion.

Regardless of whether the transmitted power P of the line is too large or the maximum power limit $P_{\max}$ of the line is too small, it can be reflected as the congestion of the transmission channel in terms of the power flow distribution. Properly distinguishing between these two situations is an important basis for selecting the relaxation variables of power flow in the specified injection space.

3.2. Generating of Transmission Congestion Channel

Finding transmission congestion channels in a power system network and adjusting the system injection power are the keys to power flow convergence adjustment. This paper estimates the initial power flow distribution based on the intermediate power flow and generates transmission congestion channels accordingly.

The depth-first search (DFS) algorithm is an important method in graph theory, as introduced in [22], and it was used in this paper for congestion channel construction.

It is worth noting that the congested channels reflect the power imbalance in the network, where a large amount of power needs to be transmitted outward near the channel sending side, while there is a significant power shortage in the area near the channel receiving side. The size of the threshold has a certain influence on the generation of congested channels. If the threshold is too large, the generated channels cannot reflect the power balance of the network. If the threshold is too small, the electrical distance of the generated congestion channels is small, which leads to insignificant power flow adjustments. Through a large number of experiments, it has been shown that a threshold value of around 0.3 is generally reasonable. Therefore, in this paper, the threshold value was set to 0.3.

4. Convergence Adjustment Method Based on Intermediate Power Flow

Due to the proximity of the injection points, the transmission congestion channels of the closest intermediate power flow can reflect the weak characteristics of the initial network flow distribution.

According to the analysis of the mechanism of power flow convergence failure, the causes of congestion are either excessive transmission power or insufficient limit power of the transmission line. When the transmission indicator is less than 0, the transmission power P_l of the line is greater than $\overline{P}_{\max}$, indicating that the congestion of the channel is caused by excessive transmission power P_l. If the indicator is greater than 0 and smaller than 0.3, it is considered that the congestion is caused by a small $\overline{P}_{\max}$. In other words, reactive power is the major cause of power flow convergence failure.

It can be concluded that the adjustment of power flow convergence failure can be made from two aspects: increasing the maximum transmission power of the congested channels and reducing the power transmission through the congested channels.

4.1. Adjustment Method to Reduce the Active Power of Congested Channels

When the injected active power of a bus greatly exceeds the maximum capacity of the transmission line, there will be a phenomenon of excessive active power in the transmission line, and it is necessary to adjust the active power of the source-load node in the channel to reduce the transmitted power.

When the line is congested, a large amount of power needs to be transmitted to the receiving end through the transmission line. The excessive active power from the sending side of the channel exceeds the capacity of the transmission line, which reflects the unreasonable arrangement of active power in the network. The sending side of the congested channel is usually a generation bus, which is referred to as the congested source bus in this paper. The unreasonable active power output of the generator at this bus causes transmission congestion, and the injected active power of this bus needs to be reduced. There is a shortage of active power on the channel receiving side, and the injected active power on the receiving side needs to be increased. The adjustment of active power follows the principle of reverse equal adjustment, that is, reducing the active power of the sending side of the channel and adding an equal amount of active power to the receiving side. Through the adjustment of active power, the power flow distribution is improved. The transmission congestion channel is shown in Figure 3. The red arrows in the diagram represent congestion channel.

The power flow congestion channels indicate a situation where a large amount of power is transmitted outward near the channel sending side and there is insufficient power stored near the receiving side. Therefore, it is necessary to adjust the power on the sending and receiving sides. Based on the active power flow passing through the sending side of the transmission line, the active power output reduction at the sending bus e and the active power adjustment at the receiving bus can be calculated using Equation (11):

$$P_e^- = \sum P_i^+ = \sum K_i (P_{lh} - \overline{P}_{lh\max}) \tag{11}$$

where P_{lh} is the active power transmitted through the first branch on the sending side of the congested channel, $\overline{P}_{lh\max}$ is the maximum transmission power capacity of the corresponding branch, P_e^- is the active power reduced by the source-bus generator, P_i^+ is the active power increased by the receiving bus, and K_i is the power distribution coefficient that is defined in Equation (12).

$$K_i = \frac{P_{hi}}{P_{hi} + P_{hj}}, i \in \{k, j\} \tag{12}$$

The physical meaning of the distribution factor in Equation (12) is that the power reduction on the channel sending side is proportionally shared by the power transmitted on the channel receiving side.

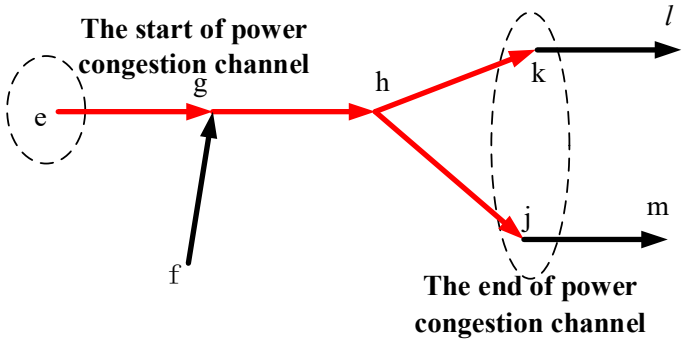

Figure 3. Diagram sketch of congestion channel.

4.2. Adjustment Method for Increasing P_{max} of Congested Channels

When there is a reactive power shortage or local reactive power imbalance in the system, the reactive power transmitted through the congested channel is too large, causing the voltage of buses in the channel to be too low, which leads to a smaller maximum power limit $P_{\max}$ of the transmission line. By performing reactive power compensation on the buses in the channel to maintain the voltage at a certain level, the maximum capacity of the transmission line can be improved, thereby improving the convergence of the power flow.

Neglecting the effect of resistance, assuming that the voltage at the sending bus remains constant during reactive power compensation, and the voltage at the receiving bus rises to a certain value, the reactive power transmitted by the transmission line after compensation can be defined as in Equation (13):

$$Q' = \frac{U_1(U_1 - U_2)}{X} \tag{13}$$

The reactive power compensation amount at the receiving bus can be calculated as $\Delta Q = Q' - Q$. When the power flow does not converge, a power flow convergence adjustment strategy based on intermediate power flow is proposed. The strategy generates transmission congestion channels based on the power distribution of intermediate power flow, determines the reasons for non-convergence according to the line transmission indicators, determines the adjustable variables, and calculates the adjustable values to improve the system power flow distribution, thereby improving the convergence of the power flow calculation. The flowchart of the power flow convergence adjustment process is shown in Figure 4.

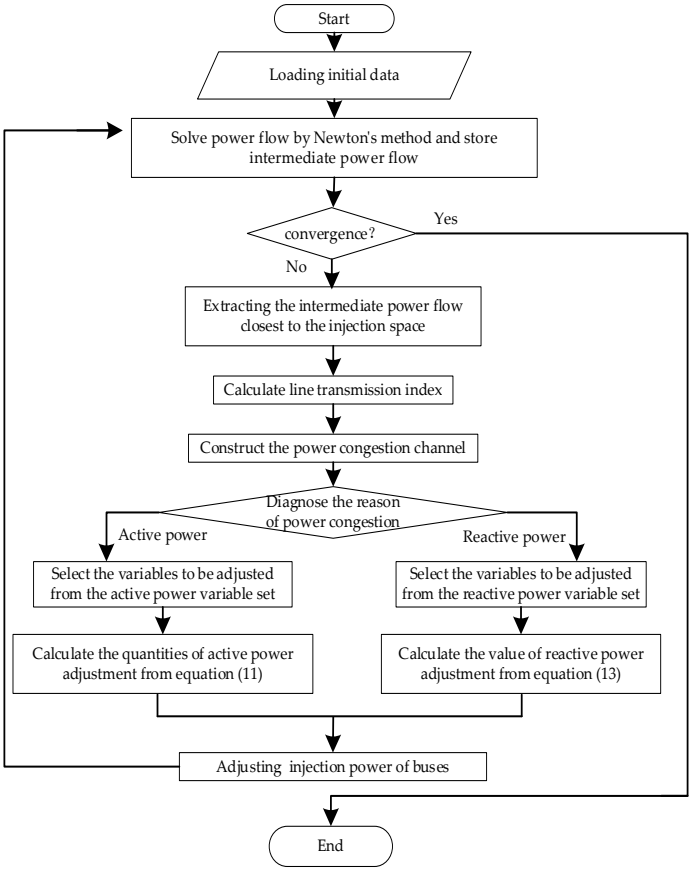

Figure 4. Flow chart of power flow adjustment.

5. Case Study

The effectiveness of the proposed method was verified through case studies using the actual power system model from a certain region utility and the European 13,659-bus system.

5.1. Actual Power Grid Simulation Case

A real power grid simulation model of a certain province in China with a voltage level of 220 kV and above was selected for the case study. The grid has 177 buses, and all variables were calculated in per unit values, with a power base of 100 MVA and a voltage base of the rated voltage at each voltage level. The maximum iteration number for power flow calculation was set to 20.

(1) Case 1: convergence failure caused by active power

By increasing the load power of all nodes to 2.5 times of their original value, non-convergent power flow was obtained. The minimum error was achieved in the 4th iteration during the iteration process, and the maximum value of the error $|\Delta F|$ in each iteration is shown in Figure 5.

As can be seen from Figure 5, the calculation error rapidly decreased and reached its minimum value in the first four iterations. After that, the error showed a trend of oscillation and divergence. Each iteration had already approached the initial power flow injection space, but the power flow could not converge completely to the initial data. The errors of each bus in the intermediate power flow are shown in Figure 6.

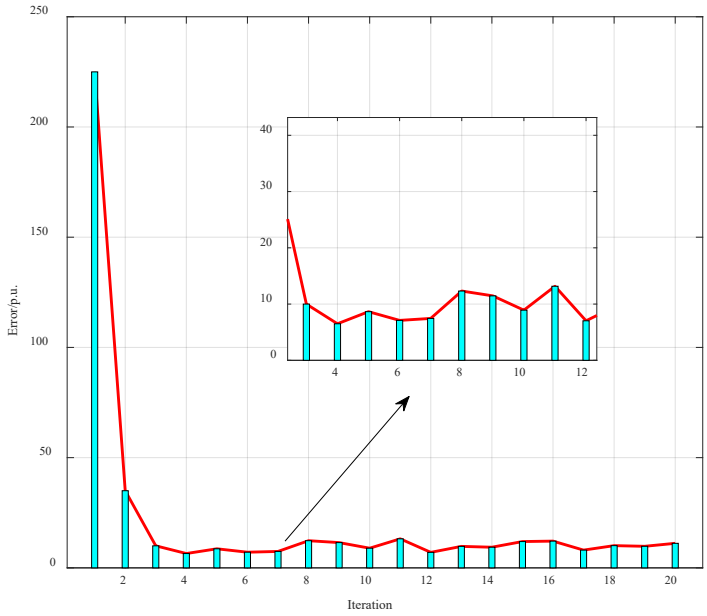

Figure 5. Iterative error in power flow calculation process.

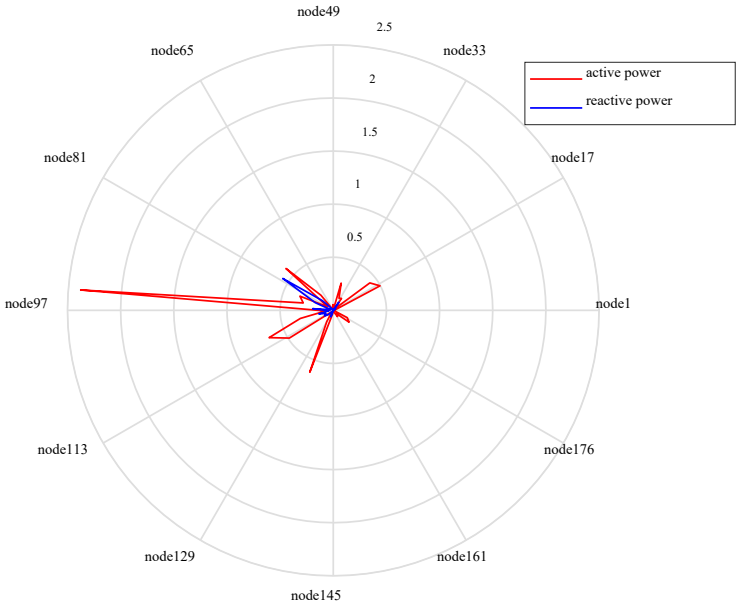

Figure 6. Intermediate power flow power error.

According to Figure 6, the injected power errors of most buses in the intermediate power flow were already small enough compared to the initial injection errors, except for a few buses with large errors. Thus, it could be concluded that the intermediate power flow was sufficiently close to the initial space, and the power flow distribution under the approximate initial injection data could be calculated based on the intermediate power flow. The transmission metrics of the lines could be calculated based on the intermediate power flow. Assuming that the line number is represented by the number of beginning bus and the number of end bus, and the line with the minimum transmission metric was line 15–18 with a metric value of −0.116. In total, five congested channels starting with line 15–18 were generated, as shown in Figure 7.

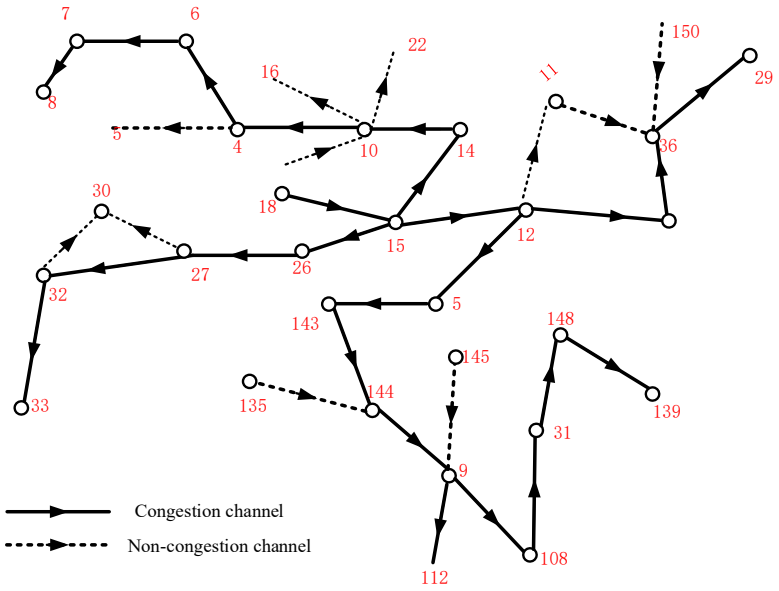

Figure 7. Intermediate power flow congestion channel in Case 1.

From the identified congestion channels, the starting line of all the congested channels was line 15–18, indicating that a large amount of active power was transmitted outward through line 15–18. This reflects a severe imbalance of active power in the area, far exceeding the transmission limit of the line. The injection power of Bus 18 was reduced, and the injection power of the receiving bus of the congested channel was increased by equalizing the sending and receiving buses of the generated congestion channel. The adjustment values calculated using Equation (11) are shown in Table 1.

Table 1. Active power adjustment results.

Channel No.	Selected Bus	Congestion Channel		Adjustment Values (p.u)
		From Bus	To Bus	
1	8	18	8	13.247
2	33	18	33	12.81
3	112	18	112	4.631
4	139	18	139	2.36
5	29	18	29	1.68

After re-performing the power flow calculation, the power flow converged again. However, if the reactive power adjustment was only performed on the buses with a lower voltage in the congested channels, the power flow could not converge. The transmission metric values of each line before and after adjustment are shown in Figure 8.

In fact, the reason for this phenomenon is that Bus 18 was a slack bus in the power system. As the load power was increased in this simulation, to ensure the active power balance of the entire system, the slack bus needed to generate a large amount of active power that far exceeded the maximum capacity of the transmission line, resulting in non-convergence of the power flow. Therefore, simply increasing the line transmission capacity through reactive power adjustment could not converge the power flow. On the contrary, reducing the active power of Bus 18 through the active power adjustment was able to reduce the active power transmitted in the congested channel and ultimately achieve a convergent power flow.

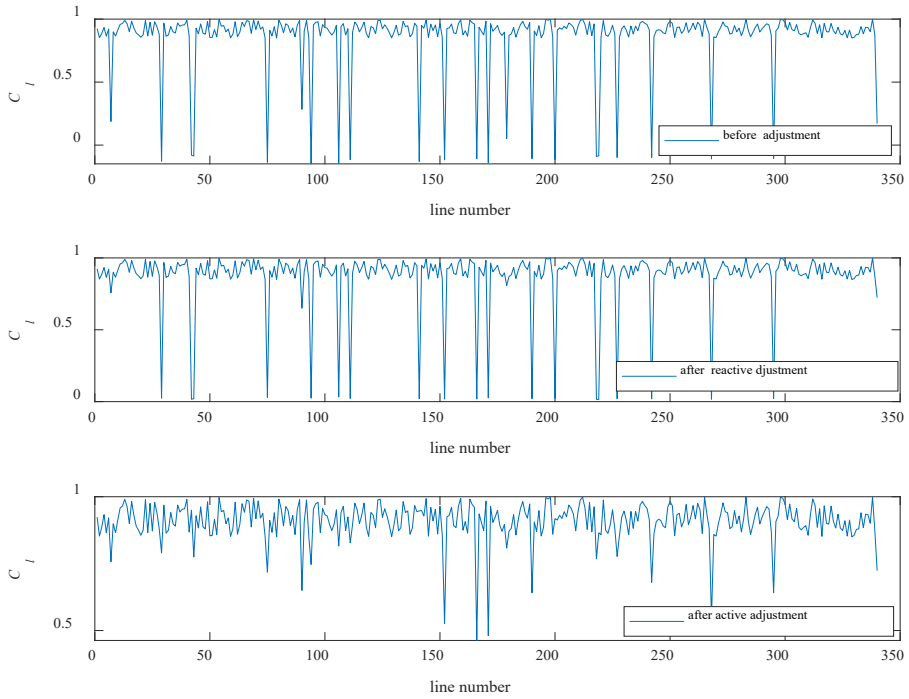

Figure 8. Line transmission metric before and after adjustment in Case 1.

(2) Case 2: convergence failure caused by reactive power

Although the active load and generation of the entire system are in a balanced state, the power flow may still not converge due to unreasonable reactive power arrangements in the power system. To simulate the power flow non-convergence caused by unreasonable reactive power arrangements, the system load was doubled, and the additional load and grid losses were borne proportionally to the output power of the generators. According to the power flow calculation, the iterative errors of each bus in the intermediate power flow are arranged from large to small in Table 2.

Table 2. Intermediate power flow iteration error.

Bus No.	Active Power (p.u)	Bus No.	Reactive Power (p.u)
99	−1.175	100	2.068
100	−1.093	140	0.389
94	−0.352	94	0.344
90	0.260	158	0.161
93	0.211	93	0.153
73	0.202	13	0.146
143	0.172	161	0.092
161	0.127	72	0.089
...	...	...	...

According to the intermediate power flow distribution, a total of four congested channels were generated, as shown in Figure 9.

Table 2 shows that the reactive power error of Bus 100 in the intermediate power flow was the largest power error in the entire system. In addition, line 94–100 had the smallest transmission metric value in the system, with a transmission metric value close to 0, indicating that the active power transmitted by the line was close to the transmission limit, and the terminal voltage of the branch was low. It can be determined that the power flow did not converge mainly due to the reactive power. Therefore, a reactive power adjustment was used to improve the transmission capacity of the line. The bus with a lower voltage on the congested channel was selected for reactive power compensation, and the

compensation amount was calculated using Equation (13). After re-calculating the power flow, the power flow converged. The results of the reactive power adjustment are shown in Table 3.

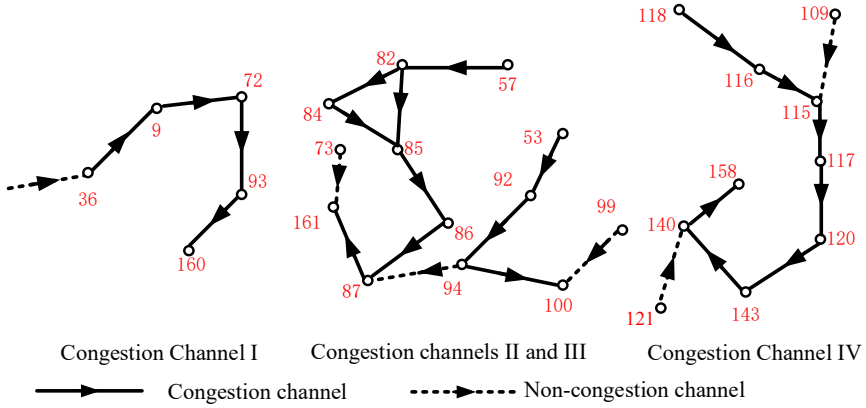

Figure 9. Intermediate power flow congestion channel in Case 2.

Table 3. Reactive power adjustment results.

Bus No.	Congestion Channel		Strategy	Adjustment Value (p.u)
	From Bus	To Bus		
93	36	160	increase	0.684
160	36	160	increase	0.320
161	57	161	increase	2.90
100	53	100	increase	3.035
94	53	100	increase	0.268
140	118	140	increase	0.358
158	118	158	increase	0.842

The transmission metric values of the lines before and after the adjustment are shown in Figure 10.

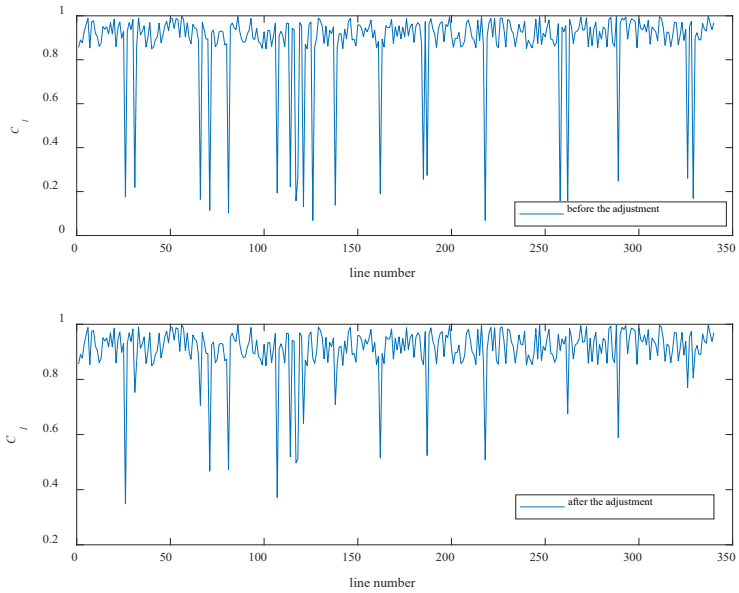

Figure 10. Line transmission metric before and after adjustment in Case 2.

As shown in Figure 10, the reactive power adjustment effectively alleviated the congestion situation of the transmission line. In fact, the reactive power adjustment increased the maximum capacity of the transmission line by raising the bus voltage magnitude. The voltage magnitudes before and after adjustment are shown in Figure 11. After adjustment, the voltage quality of the buses improved, and the voltage of all buses exceeded 0.85 p.u.

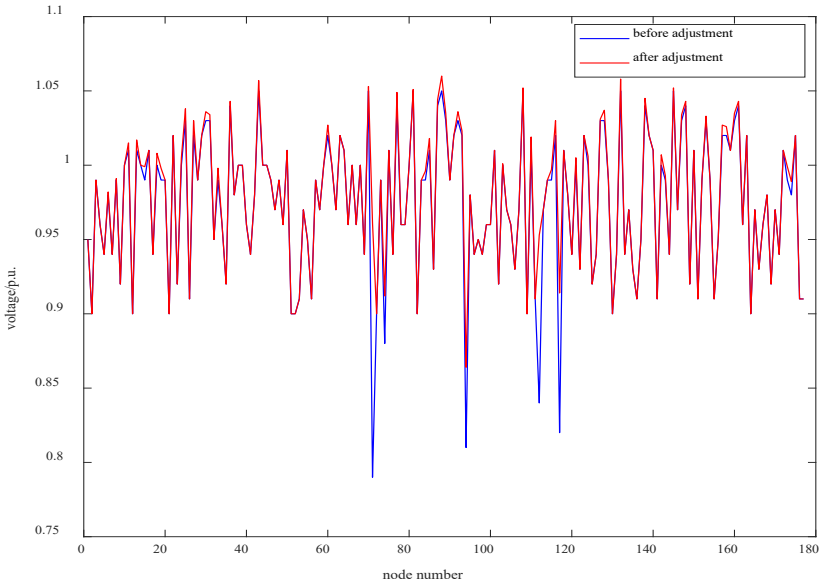

Figure 11. Voltage before and after adjustment.

As can be seen from the above two cases, the line transmission metric can be used to accurately identify the causes of power flow convergence failure and provide guidance for power flow adjustment.

5.2. Simulation Cases in Bulk Power Systems

To verify the effectiveness of the proposed method in bulk power systems, the simulations in this section were performed using the European 13,659-bus system. The system contains 4092 generators, 9567 PQ buses, and 20,467 branches, with the buses divided into 24 regions. The generation and load data of each bus in Region 2 were multiplied by a random coefficient within the range of [0.8, 1.2], resulting in power flow convergence failure.

After performing the power flow calculation with the initial data, the power flow calculation did not converge when it reached the maximum iteration. The closest intermediate power flow was generated from the 8th iteration. The maximum capacity of the transmission line based on the intermediate power flow was calculated. There were 26 active power and 11 reactive power congestion channels in the grid, and 183 key variables were identified, among which 129 active power variables and 54 reactive power variables needed to be adjusted. Therefore, active power and reactive power adjustments were performed simultaneously. Based on the congested channels generated in the intermediate power flow, the adjustment variables were determined, and the initial data were adjusted accordingly. The adjusted results are shown in Table 4. After re-calculating the power flow with the adjusted injection data, convergence was achieved after four iterations.

After adjustment, the average voltage of Region 2 was increased from 0.823 p.u. to 0.945 p.u., and the voltage level of the perturbation region obviously improved. The transmission margin of line 1597–1585, i.e., the line with the lowest transmission margin in the system, was increased from 0.061 to 0.375, and the power blocking situation of the whole network was significantly improved. In addition, the active power output of some generators with power exceeding the limit in Region 2 returned to a reasonable range.

Table 4. Multi-power adjustment results.

Bus No.	Variable Type	Strategy	Adjustment Value/p.u.
405	active power	increase	0.237
470	active power	increase	0.082
4254	active power	increase	0.180
1350	reactive power	increase	0.161
6651	active power	increase	0.375
342	active power	decrease	0.228
12,273	reactive power	increase	0.147
13,254	active power	decrease	0.972
412	reactive power	decrease	0.028
1142	reactive power	decrease	0.044
3277	reactive power	decrease	0.116
4452	active power	decrease	0.218
4619	active power	decrease	0.022
5058	active power	decrease	0.381
11,332	active power	decrease	0.181
...	...	...	...

The results indicate that the proposed method is applicable in this bulk power system. Compared with the algorithms based on optimization models, the proposed method is completely based on iterative data, which avoids complex modeling and problem-solving processes. It fully utilizes the non-convergence information explored by the intermediate power flow, which provides guidance for solving the power flow non-convergence problem.

6. Conclusions

1. An analysis of the mechanism of power flow convergence failure from the perspective of power transmission congestion was conducted, and theoretical guidance for studying power flow convergence failure is proposed;
2. Based on the intermediate data from the power flow iteration, the index of transmission power congestion was constructed, and a method for identifying congested channels is proposed to diagnose the causes of power flow convergence failure;
3. A correction strategy for power flow injection space data was designed with the aim of alleviating transmission channel congestion, which generates relaxation schemes for operational variables;
4. The proposed strategy was tested using an actual power grid and a standard example power system with 13,659 buses. The simulation results show that the bus voltage magnitude was improved to better meet the operational requirements. The value of the power congestion index obviously increased after applying the proposed adjustment scheme;
5. The method proposed in this paper can be entirely based on intermediate data of the power flow iteration, which avoids complex power flow adjustment modeling and provides methodological support for power flow diagnosis in bulk power systems.

7. Research Prospects

The method proposed in this paper can diagnose the reasons for the non-convergence of power flow in bulk power systems from both a theoretical and simulation perspective. Our method is suitable for adjusting the non-convergence of power flow in engineering practice. However, only offline data were used for method verification in this study. In the future, the method will be applied to online diagnoses in order to ensure the safe operation of the power grid.

Author Contributions: Conceptualization, G.M.; methodology, G.M., Y.Z. and M.Y.; validation, J.C.; writing—original draft, G.M. and Y.Z.; writing—review & editing, M.Y. and J.C. All authors have read and agreed to the published version of the manuscript.

Funding: This research was funded by National Natural Science Foundation of China (grant number 51877034).

Data Availability Statement: Not applicable.

Conflicts of Interest: The authors declare no conflict of interest.

References

1. Wang, W.; Shi, W. Application of new power flow calculation in ship power system. *J. Phys. Conf. Ser.* **2023**, *2450*, 012089. [CrossRef]
2. Xiao, H.; Pei, W.; Wu, L.; Ma, L.; Ma, T.; Hua, W. A novel deep learning based probabilistic power flow method for Multi-Microgrids distribution system with incomplete network information. *Appl. Energy* **2023**, *335*, 120716. [CrossRef]
3. Grisales-Noreña, L.F.; Morales-Duran, J.C.; Velez-Garcia, S.; Danilo, M.O.; Walter, G.-G. Power flow methods used in AC distribution networks: An analysis of convergence and processing times in radial and meshed grid configurations. *Results Eng.* **2023**, *17*, 100915. [CrossRef]
4. Quintana, E.; Inga, E. Optimal Reconfiguration of Electrical Distribution System Using Heuristic Methods with Geopositioning Constraints. *Energies* **2022**, *15*, 5317. [CrossRef]
5. García, J.; Inga, E. Georeferenced rural distribution network model considering scalable growth of users in rural areas. *Heliyon* **2023**, *9*, e12724. [CrossRef] [PubMed]
6. Tang, K.; Dong, S.; Zhu, B.; Song, Y. Performance analysis and improvement of Newton method for power flow calculation of large-scale integrated transmission and distribution network. *Autom. Electr. Power Syst.* **2019**, *43*, 92–99. [CrossRef]
7. Costilla-Enriquez, N.; Weng, Y.; Zhang, B. Combining Newton-Raphson and Stochastic Gradient Descent for Power Flow Analysis. *IEEE Trans. Power Syst.* **2021**, *36*, 514–517. [CrossRef]
8. Steinegger, J.; Wallner, S.; Greiml, M.; Kienberger, T. A new quasi-dynamic load flow calculation for district heating networks. *Energy* **2023**, *266*, 126410. [CrossRef]
9. Ding, T.; Li, C.; Yang, Y.; Bo, R.; Frede, B. Negative Reactance Impacts on the Eigenvalues of the Jacobian Matrix in Power Flow and Type-1 Low-Voltage Power-Flow Solutions. *IEEE Trans. Power Syst.* **2016**, *32*, 3471–3481. [CrossRef]
10. Valenzuela, A.; Simani, S.; Inga, E. Automatic Overcurrent Protection Coordination after Distribution Network Reconfiguration Based on Peer-To-Peer Communication. *Energies* **2021**, *14*, 3253. [CrossRef]
11. Sun, X.; Rao, Y.; Xiao, H.; Li, C.; Ruan, Z. Available transfer capability calculation based on linearized optimal power flow. *Electr. Power Autom. Equip.* **2020**, *40*, 194–199. [CrossRef]
12. Milano, F. Analogy and Convergence of Levenberg's and Lyapunov-Based Methods for Power Flow Analysis. *IEEE Trans. Power Syst.* **2016**, *31*, 1663–1664. [CrossRef]
13. Lu, W.; Liu, M.; Lin, S.; Li, L. Fully Decentralized Optimal Power Flow of Multi-Area Interconnected Power Systems Based on Distributed Interior Point Method. *IEEE Trans. Power Syst.* **2018**, *33*, 901–910. [CrossRef]
14. Shestakova, V.; Kats, I.; Darkhanova, A. Power flow calculations in power systems considering traction load. *Mater. Sci. Eng.* **2021**, *1019*, 012004. [CrossRef]
15. Iwamoto, S.; Tamura, Y. A fast load flow method retaining Nonlinearity. *IEEE Trans. Power Appar. Syst.* **1978**, *PAS-97*, 1586–1599. [CrossRef]
16. Iwamoto, S.; Tamura, Y. A Load Flow Calculation Method for Ill-Conditioned Power Systems. *IEEE Trans. Power Appar. Syst.* **1981**, *100*, 1736–1743. [CrossRef]
17. Li, M.; Chen, J.; Chen, H.; Duan, X. Load flow regulation for unsolvable cases in a power system. *Autom. Electr. Power Syst.* **2006**, *30*, 11–15.
18. Wang, Y.; Hou, J.; Ma, S.; Zheng, C.; Xu, X. A method of automatic integration and regulation of power flow data for security and stability check of generation scheduling analysis. *Power Syst. Technol.* **2010**, *34*, 100–104. (In Chinese) [CrossRef]
19. Peng, H.; Yuan, H.; Bao, Y.; Li, F. Identification and correction method for ill-conditioned power flow of large scale network. *Power Syst. Prot. Control* **2018**, *46*, 116–123. [CrossRef]
20. An, J.; Song, J.; Ge, W. Convergence identification and adjustment method for power flow calculation in large power grid. *Electr. Power Autom. Equip.* **2020**, *400*, 103–109. [CrossRef]
21. Peng, H.; Li, F.; Yuan, H.; Bao, Y. Power Flow Calculation and Condition Diagnosis for Operation Mode Adjustment of Large-scale Power Systems. *Autom. Electr. Power Syst.* **2018**, *42*, 136–142. [CrossRef]
22. Alamsyah; Amir, A.; Subito, M.; Fauzi, R.; Amirullah. Performance analysis of breadth-first search and depth-first search on MANET for health monitoring system. *Earth Environ. Sci.* **2022**, *1075*, 012011. [CrossRef]